Growth and Morphology of Mesoporous SBA-15 Particles

Peter Linton and Viveka Alfredsson*

Physical Chemistry 1, Lund University, P.O. Box 124, SE-221 00 Lund, Sweden

Received November 28, 2007
Revised Manuscript Received March 11, 2008

Mesoporous silica SBA-15[1] is formed under aqueous acidic conditions using nonionic triblock copolymers (Pluronics) as structure directing agents. There is an increasing interest in understanding how the formation of mesoporous materials proceeds.[2,3] Knowledge of this kind is important to provide the necessary means for controlling and directing the formation of mesoporous materials. Structure, particle morphology,[4,5] and size distribution are all material properties that need to be monitored for application purposes. Hence, an understanding of the events controlling particular growth as well as structure maturing is imperative.

Here we report on the growth progression of particles of mesoporous silica with the SBA-15 structure. The data are based on observations made by transmission electron microscopy. Previously we,[6,7] as well as others,[8–11] have reported on the structural transformation of a globular micellar−silica composite to a hexagonal structure. In this work our attention is devoted to the dynamics of the micellar aggregation and how this affects particle size and particular growth. The material obtained is a highly ordered 2D hexagonal (*p*6*mm*) structure.

SBA-15 was synthesized with Pluronic P104 ($(EO)_{27}$-$(PO)_{61}$-$(EO)_{27}$) as structure director and with HCl (1.6 M) as the acid medium. Synthesis parameters are based on the normal SBA-15 synthesis[1] but with P104 used instead of the more frequently used P123. Tetramethyl orthosilicate (TMOS) was used as the silica source (98%). The reagent solution had the following composition by weight P104/H_2O/HCl (4.0 M)/TMOS 1/23.44/15.62/1.52. Prior to addition of TMOS the other reagents were mixed and tempered to the specified temperature (50°, 55°, 60°, and 65 °C respectively). After addition of the silica source the solution was left stirring on the bench at the specified temperature for 24 h.

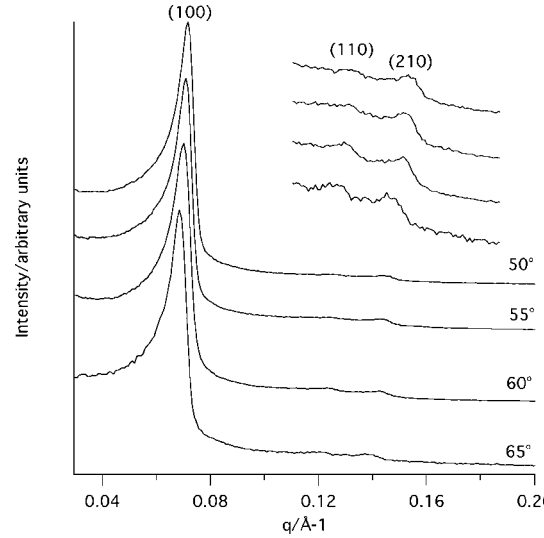

Figure 1. SAXS patterns of the material synthesized at the four different temperatures. These materials have also been hydrothermally treated and calcined. Top right: enlargement of the corresponding higher order peaks. (The width of the peaks is determined by instrumental parameters and not particles size).

Electron micrographs were recorded with a JEOL 3000F (300 kV) or a Philips (120 kV) transmission electron microscope, and the materials were dispersed on holey carbon copper grids. Small angle X-ray scattering was performed on a kratky camera equipped with a position sensitive detector.

SBA-15 formed in the temperature interval 50−65 °C under the conditions mentioned above are highly ordered with unit cell parameter for the calcined material of 101.0 Å (50 °C synthesis) and 105.8 Å (65 °C synthesis). See the XRD pattern in Figure 1. The particles formed are single crystals and in many respects similar to hexosome particles formed in self-assembled lipid systems.[12] The particle size and crystal habit vary as a function of temperature, but for each temperature the particle size is uniform and the crystal habit is well defined. In general, the particle size increases with a temperature decrease. The size increase is the result of a dual effect that will be explained below. The electron micrograph in Figure 2b shows the result of a synthesis performed at 55 °C. The particles made at this temperature have an unusual form (average particle size: diameter, 0.97 μm; height, 0.43 μm). The crystal habit is that of a hexagonal prism, an atypical morphology for SBA-15,[5,13] although there are wedges missing for a perfect shape. The particle seems to be made up of seven smaller particles (Figure 3). At 50 °C (Figure 2a) the same effect, however less pronounced, is observed. At this temperature the missing wedges are

* To whom correspondence should be adressed.

(1) Zhao, D.; Huo, Q.; Feng, J.; Chmelka, B. F.; Stucky, G. D. *J. Am. Chem. Soc.* **1998**, *120*, 6024–6036.
(2) Edler, K. *Aust. J. Chem.* **2005**, *58*, 627–643.
(3) Wan, Y.; Zhao, D. *Chem. Rev.* **2007**, *107*, 2821–2860.
(4) Park, S. S.; Lee, C. H.; Cheon, J. H.; Park, D. H. *J. Mater. Chem.* **2001**, *11* (12), 3397–3403.
(5) Zhang, H.; Sun, J.; Ma, D.; Weinberg, G.; Su, D. S.; Bao, X. *J. Phys. Chem. B* **2006**, *110*, 25908–25915.
(6) Flodström, K.; Wennerström, H.; Alfredsson, V. *Langmuir* **2004**, *20*, 680–688.
(7) Flodström, K.; Teixeira, C. V.; Amenitsch, H.; Alfredsson, V.; Lindén, M. *Langmuir* **2004**, *20*, 4885–4891.
(8) Ruthstein, S.; Frydman, V.; Kababya, S.; Landau, M.; Goldfarb, D. *J. Phys. Chem. B* **2003**, *107*, 1739–1748.
(9) Ruthstein, S.; Frydman, V.; Goldfarb, D. *J. Phys. Chem. B* **2004**, *108*, 9016–9022.
(10) Khodakov, A. Y.; Zholobenko, V. L.; Imperor-Clerc, M.; Durand, D. *J. Phys. Chem. B* **2005**, *109*, 22780–22790.
(11) Ruthstein, S.; Schmidt, J.; Kesselman, E.; Talmon, Y.; Goldfarb, D. *J. Am. Chem. Soc.* **2006**, *128*, 3366–3374.
(12) Barauskas, J.; Johnsson, M.; Tiberg, F. *Nano Lett.* **2005**, *5*, 1615–1619.
(13) Zhang, H.; Sun, J.; Ma, D.; Bao, X.; Klein-Hoffmann, A.; Weinberg, G.; Su, D.; Schlögl, R. *J. Am. Chem. Soc.* **2004**, *126*, 7440–7441.

10.1021/cm703375p CCC: $40.75
Published on Web 04/10/2008

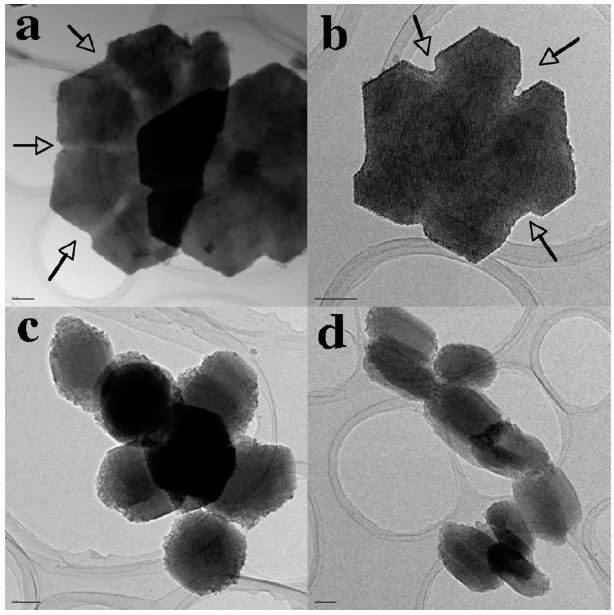

Figure 2. Electron micrographs of the particles formed at (a) 50, (b) 55, (c) 60, and (d) 65 °C. Scale bars: 200 nm. Arrows pointing at less dense areas (a) and missing wedges (b).

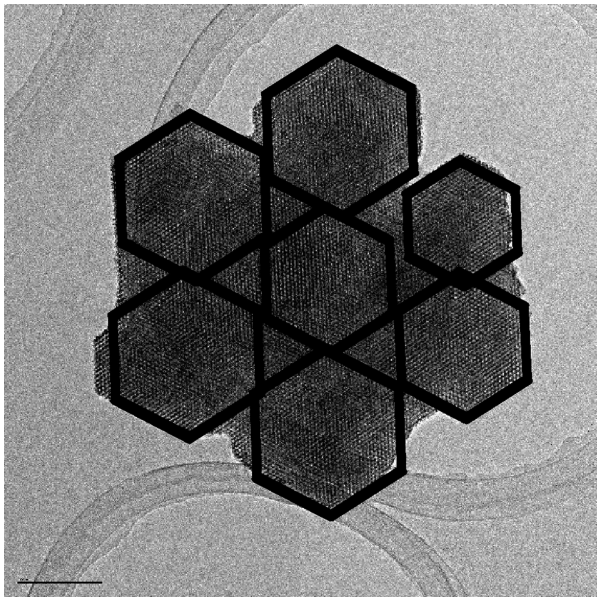

Figure 3. Electron micrograph of a particle synthesized at 55 °C. Inserted are hexagons of approximate primary particles. Scale bar: 200 nm.

replaced by less dense areas which in certain cases also contain small holes in the structure. The particle size also differs. The 50 °C particles are larger (diameter, 1.75 μm; height, 0.40 μm). A higher temperature (60 °C) on the other hand gives smaller and defect-free particles (Figure 2c; diameter, 0.55 μm; height, 0.53 μm). Yet another 5 °C raise in temperature gives even smaller, still defect-free, particles (Figure 2d; diameter, 0.38 μm; height, 0.68 μm).

The formation of mesoporous silica is initiated when the silica source is added to the micellar solution. Our previous investigations of the formation of SBA-15 have demonstrated that the initial globular micellar solution aggregates as the silica polymerization progresses, leading to a subsequent reorganization to a 2D hexagonal structure due to the positive interaction between the siliceous species and the EO groups of the structure-directing polymer.[6,7] Here our focus is on the growth mechanism of the particles. In the syntheses we obtain particles with well-defined morphologies and highly uniform particle sizes. The particle habit can be understood as a result of the nucleation and growth processes explained by the four steps described below. It is essential that these steps occur in sequence and not in parallel. The latter would produce large size variation of the particles.

1. Initial Aggregation. The aggregation of micelles is a consequence of micellar collisions. This can be described by the reaction $M_1 + M_{n-1} \leftrightarrow M_n$, where M_1 represent a single micelle (consisting of Pluronic molecules with attached siliceous monomers/oligomers) and M_n a group of n micelles. Initially the reaction will in general not lead to an association, but with time, likely as a consequence of the ongoing silica polymerization, the forward reaction will be favored. At a certain time the saturation point is reached, although there is a nucleation barrier[14] that needs to be passed in order for energetically stable aggregates to form. Eventually, as silica polymerization proceeds, this barrier will be passed and the nucleation process is initiated.

2. Nucleation. The nucleation will last for a limited time and result in a number of nuclei. To obtain a monodisperse size distribution of the particles it is essential that the nucleation step occurs in a single short burst.[14–16] The number of nuclei that is formed determines the number of (primary) particles.

3. Growth of Primary Particles. The nuclei will grow and essentially all the micelles will eventually be consumed. This will lead to larger primary aggregates, with N micelles where N is in the range 10^4 micelles. The aggregates will develop an internal 2D hexagonal mesophase[6,7] and, as this phase is anisotropic, the aggregates will have an anisotropic equilibrium form. We have observed that this form is dependent on the synthesis temperatures. At 65 °C the particles are elongated; hence, the (001) faces are energetically less favorable. At 55 and 50 °C the particles are flat hexagonal prisms indicating unfavorable (100) and ($\bar{1}$00) faces. The particles formed at 60 °C have an intermediate form.

4. Association of Primary Particles. The primary particles can also associate. At the higher temperatures (60 and 65 °C), where the silica polymerization is faster, this association is controlled by weak van der Waals interaction and the identity of the primary particles are, as noted (Figure 1 c,d), preserved. However, at the lower temperatures (50° and 55 °C) the association is stronger, likely due to incomplete silica polymerization. Here it is observed that the final particles are composed of aggregates of several primary particles (Figure 2a,b). The primary particles aggregate, in general, in groups of seven, like in Figure 3, an aggregate that provides an energetic minimum. If on the other hand the aggregation is hindered by diluting the synthesis solution at a specific time, with equal amounts of 1.6 M HCl at 55 °C, primary particles are obtained. The primary particles

(14) Evans, D. F.; Wennerström, H. *The colloidal domain: where physics, chemistry and biology meet*, 2nd ed.; Wiley-VCH: New York, 1999.
(15) Goia, D. V.; Matijevíc, E. *Colloids Surf., A* **1999**, *146*, 139–152.
(16) Privman, V.; Goia, D. V.; Park, J.; Matijevíc, E. *J. Colloid Interface Sci.* **1999**, *213*, 36–45.

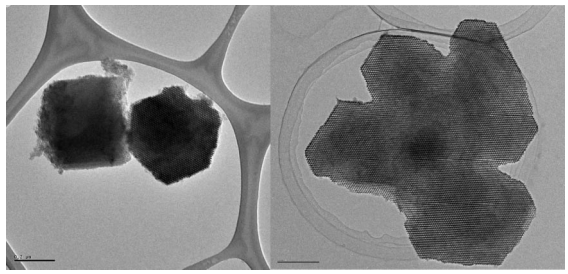

Figure 4. Electron micrograph of primary particles made at 55 °C (left) by diluting the synthesis, and the corresponding secondary particle (right) from a normal synthesis. Note that the secondary particle in this case lacks its seventh primary particle. Scale bars: 200 nm.

(Figure 4) are monodisperse, well-ordered, and have the same size as the identified primary particles in the secondary structure. The diameter and the height of the primary particles are both about 0.46 μm. The final secondary particles are single (mesoscopic) crystals. Hence the interface between the primary particles has healed forming an essentially structurally defect free final particle. The crystal habit of the secondary particles is a generic feature (Figure 3). Here we propose a mechanism that explains this peculiar morphology. During the formation of the primary particles the initial phase separated droplets will, as the silica polymerization proceeds, adopt a morphology reflecting the internal 2D hexagonal structure,[6] based on a hexagonal prismatic shape (see Scheme 1 in the Supporting Information). In the interim period, between a droplet and a hexagonal prism, some energetically unfavorable faces will be expressed. These faces will not be present when the structure has matured. We suggest that the association between primary particles arises when these energetically unfavorable faces combine, prior to the final hexagonal prismatic shape being attained. Hence, the primary particles will fuse along crystallographically equivalent faces with the same orientation (see Scheme 2 in the Supporting Information), thus enabling the formation of the structurally defect free particles. However, there will be some empty spaces between the associated primary particles. These areas will to some extent be filled with material as the structure at this stage is not rigid but rather in the course of maturing. This process is however not faultless and holes and crevices are generally occurring features in the particles obtained under the conditions of the syntheses used here. We have never observed particles with a morphology consistent with association of the initial spherical droplets, and this indicates that for association to occur some ordering in the particles is essential. Neither is any association along the (001) faces observed for these syntheses although other conditions may instigate such aggregation.[5] This particle growth effect may be a general mechanism for the growth of mesoporous material and not restricted to these particular synthesis conditions. Albeit to observe this effect the conditions are restricted. For instance, if the synthesis here reported is carried out at lower temperatures, the interfaces betewen primary particles are no longer visible. A similar growth behavior was observed for the zeolite analcime[17] where the early aggregation occurred by crystalline nanoplatelets aggregated into larger discs. Also in this case the primary particles (nanoplatlets) aggregated in a crystallographic orientation.

We propose a mechanism for the aggregate growth of mesosporous particles that gives insight into the steps controlling the formation of mesoporous silica particles. This mechanism is described by four steps, initial aggregation, nucleation, growth of primary particles, and finally, under certain conditions, association to secondary particles via oriented aggregation. This novel aggregation behavior that could be a generic feature for several systems provides important knowledge on how to control particle size for mesoporous materials. In addition, as the particle size can be controlled by temperature, this synthesis protocol offers an easy and straightforward way of making highly ordered SBA-15 with a well-defined particle size. The protocol also offers the possibility to form SBA-15 with the unusual morphology of plate-like hexagonal prisms.

Acknowledgment. The authors are grateful to Håkan Wennerström for insightful discussions. The Crafoord Foundation and the Colintech program of SSF are acknowledged for financial support. Financial support by the Swedish Research Council (VR) through the Linnaeus Center of Excellence on Organizing Molecular Matter (OMM) is also gratefully acknowledged.

Supporting Information Available: Schemes 1 and 2 and additional electron micrographs (PDF). This material is available free of charge via the Internet at http://pubs.acs.org.

CM703375P

(17) Chen, X.; Qiao, M.; Xie, S.; Fan, K.; Zhou, W.; He, H. *J. Am. Chem. Soc.* **2007**, *129*, 13305–13312.